12WCEE 2000

A COMPARISON OF SITE-AMPLIFICATION ESTIMATED FROM DIFFERENT METHODS USING A STRONG MOTION OBSERVATION ARRAY IN TANGSHAN, CHINA

Wenbo ZHANG[1] And Koji MATSUNAMI[2]

SUMMARY

A seismic observation array for strong motions were deployed to estimate seismic source, propagation path and local site effects in Tangshan, China. About sixty events ranging from *M* 2.2 to 5.9 were recorded in the past several years. We first separated seismic source, propagation path and local site effects from a linear inversion of S-wave spectra using the data set of 10 events recorded at 8 stations. We next compared site responses from the S-wave inversion and those from other techniques, such as traditional direct spectral ratios of S waves, receiver-function of S waves. From the separation, we found that S-wave quality factor, i.e. Q_s-value, is approximately satisfied with the relation of $Q_s = 67\, f^{1.1}$ in the range of frequency from 0.5 to 32 Hz. The source spectra follow the ω^{-2} model of seismic source for low frequencies less than about 12 Hz. From the comparison of site responses estimated by the different methods for each soil site, we found that all the methods can extract the same predominant peaks from the responses. The amplifications from direct S wave spectral ratios are well correlated with those from the S-wave inversion within a factor of 2 to 3. While the correlation between the amplifications from S-wave receiver-function and those from the S wave inversion is not good, especially for high frequencies more than 8 Hz.

INTRODUCTION

It has been known that each soil type responds differently when it is subjected to ground motion from earthquakes. So, the study of local site effects on seismic ground motions is one of the most important goals of earthquake engineering. It is practical importance to develop methods for assessing the nature and potential of sediment amplification, especially when choosing the location and design of critical and essential facilities. At present, however, the method by which site amplification is determined is still under investigation among seismologists and earthquake engineers.

A seismic observation array for strong motions was deployed in Tangshan area, China, to do basic researches for the prediction of strong ground motions. This area is seismically active. The well known two earthquakes occurred in the region: the Tangshan Earthquake (Ms = 7.8, July 28, 1976) and its largest aftershock (Ms = 7.1,July 28, 1976). The array consists of eight observation stations and one downhole observation system. About sixty events in the magnitude (M_L) range from 2.2 to 5.9 were observed in the past several years. The data set provides us an opportunity to study the local site effects empirically from the observed strong-motion records, especially in high frequency range.

The greatest challenge in estimating site responses from earthquake data is to remove the source and path effects. Simultaneous separation of source, propagation path and local site effects from strong motion records is effective for this purpose. In this paper, we used an inversion method for S waves to separate the source, propagation path and local site effects simultaneously. We also used the other methods to examine the site amplification: traditional spectral ratios of S waves and receiver function of S waves.

[1] *Institute of Engineering Mechanics, State Seismological Bureau, Harbin, China*
[2] *Disaster Prevention Research Institute, Kyoto University, Japan*

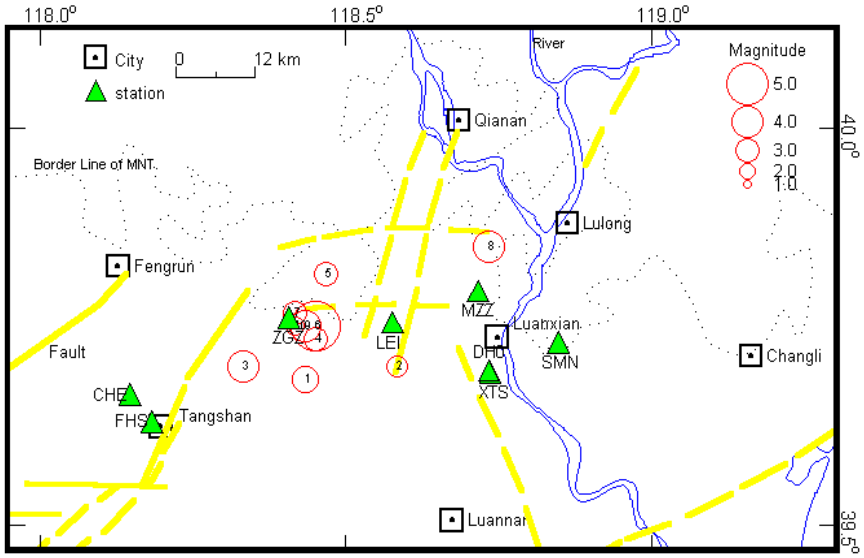

Fig.1 Map showing eight stations (▲) and ten events (O)

Table 1 Parameters for observed earthquakes and recording stations

No.	Date	Time	M	Lat.	Long.	ZGZ	MZZ	LEI	DH0	XTS	SMN	FHS	CHE
1	93/09/30	18:13:34	3.4	39°41'	118°26'	*	*		*	*			
2	95/02/07	01:51:46	2.7	39°42'	118°35'	*	*	*	*	*			
3	95/02/22	19:53:02	3.9	39°42'	118°20'	*	*	*					
4	95/06/27	22:46:19	3.0	39°44'	118°27'	*	*	*	*				
5	95/09/19	23:48:03	2.9	39°49'	118°28'	*	*		*				
6	95/10/06	06:26:57	5.9	39°45'	118°27'	*	*	*	*	*	*		
7	95/10/06	07:51:50	3.0	39°46'	118°25'	*	*	*					
8	96/04/08	00:39:29	4.0	39°51'	118°44'	*	*		*	*			
9	96/04/08	22:08:59	3.9	39°45'	118°26'	*	*		*	*			
10	97/02/28	20:43:20	3.8	39°16'	118°43'	*	*				*	*	

Table 2 Stations, instruments and site conditions

Station	Lat.	Long.	Instrument	Site Condition
ZGZ	39.761°	118.407°	CV901,Kelunji	Rock
MZZ	39.795°	118.716°	CV901	Soil
LEI	39.755°	118.576°	Kelunji	Soil
DH0	39.695°	118.734°	SSR-1	Soil
XTS	39.692°	118.736°	CV901	Rock
SMN	39.730°	118.847°	CV901	Soil
FHS	39.630°	118.183°	CV901	Rock
CHE	39.664°	118.147°	CV901	Soil

Velocity type: CV901; Acceleration type: SSR-1, Kelunji

DATA

In this study, 10 events recorded at Tangshan array were used to analyze. **Figure 1** shows the distribution of events as well as the strong-motion stations. **Table 1** lists the parameters for observed earthquakes and the recording stations. **Table 2** shows the coordinates of the stations, the instrument and the site condition of each station. For the procedure of processing the data set, first we determined the S-P time at each station for an event. We used S-P time rather than the distance calculated using catalog coordinates to estimate hypocentral distances. Then we converted acceleration to velocity by using integrating method, and resampled all the data at a sample rate of 100 Hz. A 5-sec time-window was applied to extract S waves and a 5% Hanning taper was applied to the time-windows. A time-window with a length of 2 seconds before P-wave arrival was taken to examine a noise level. The spectra of a noise and a signal were smoothed and re-interpolated by a common frequency interval, and only the data with a signal-to-noise ratio greater than two were used to analyze. During the calculation, each amplitude spectrum is defined as the root-mean-square average of two horizontal-component spectra:

$$H(f) = [\ (NS^2(f) + EW^2(f))/2\ ]^{1/2} \quad (1)$$

Here, *NS(f)* and *EW(f)* is the spectrum of N-S component and E-W component, respectively. For all the spectra, the smoothing was done using a Hanning window with a band-width of±0.5 Hz.

METHODS

A linear Inversion for S waves

For the observed S waves, its Fourier amplitude spectrum can be expressed as (Hartzell, 1992):

$$O_{ij}(f) = S_i(f)\, G_j(f)\, R_{ij}^{-1}\, exp\,(-\pi R_{ij} f / Q_s(f)\, V_s) \quad (2)$$

where, $O_{ij}(f)$ is the S-wave Fourier amplitude spectrum of the *i*th event recorded at the *j*th station; $S_i(f)$ and $G_j(f)$ are the source and site term, respectively; R_{ij} is the hypocentral distance; $Q_s(f)$ and V_s denote the average quality factor and average velocity of S waves, respectively.

Equation(2) is rewritten as:

$$G_j(f) = O_{ij}(f)\, R_{ij}\, S_i^{-1}(f) exp(\pi R_{ij} f / Q_s(f)\, V_s) \quad (3)$$

Station ZGZ was selected as the reference station in our study. So, for the ith event at ZGZ:

$$G_{zgz}(f) = O_{izgz}(f)\, R_{izgz}\, S_i^{-1}(f) exp(\pi R_{izgz} f / Q_s(f) V_s) \quad (4)$$

Ratios between the spectrum at *j*th station and that at ZGZ for the ith event:

$$G_j(f)/G_{zgz}(f) = [O_{ij}(f)/O_{izgz}(f)]\,[R_{ij}/R_{izgz}] \times exp[\pi\,(R_{ij}-R_{izgz})\, f / Q_s(f)\, V_s] \quad (5)$$

By taking the logarithm, equation (4) is rewritten at a fixed frequency as:

$$g_j^{zgz} + \pi\,(R_{izgz}-R_{ij}) f / Q_s V_s = o_{ij}^{izgz} + r_i^{zgz} \quad (6)$$

here, $g_j^{zgz} = log(G_j/G_{zgz})$, $o_{ij}^{izgz} = log(O_{ij}/O_{izgz})$, *and* $r_i^{zgz} = log(R_{ij}/R_{izgz})$.

Denote that $\pi\,(R_{izgz}-R_{ij})\, f / V_s = \alpha_{ij}$, and $o_{ij}^{izgz} + r_i^{zgz} = d_{ij.}$ So, equation (6) becomes as

$$g_j^{zgz} + \alpha_{ij} Q_s^{-1} = d_{ij} \quad (7)$$

For I events and J stations, equation (7) can be expressed in a matrix form as

$$Gm = d \quad (8)$$

The standard deviations of the model parameters were estimated from diagonal elements of the covariance matrix (Menke, 1989):

$$[covm] = \sigma_d^2\, [\, G^T G]^{-1} \quad (9)$$

where σ_d^2 is the variance of the data.

Traditional spectral ratios for S waves

Equation (2) can be rewritten in a simple form:

$$O_{ij}(f) = S_i(f) G_j(f) P_{ij}(f) \quad (10)$$

here $P_{ij}(f)$ is the path term between the *i*th event and *j*th station. Traditional spectral ratio method is calculated dividing the spectrum of a S wave at the *j*th station by that of a S wave at the reference station ZGZ:

$$O_{ij}(f)/O_{izgz} = [S_i(f) G_j(f) P_{ij}(f)]/[S_i(f) G_{zgz}(f) P_{izgz}(f)] = [G_j(f) P_{ij}(f)]/[G_{zgz}(f) P_{izgz}(f)] \quad (11)$$

The spectra of the data were corrected for geometrical spreading by multiplying each spectrum at the *j*th station for the *i*th event by its corresponding S-P time assuming that the effect of Q_s is negligible (Bonilla, et al., 1996). Thus, equation (15) becomes

$$O_{ij}(f)/O_{izgz} = [G_j(f) T_{ij}] / [G_{zgz}(f) T_{izgz}] \quad (12)$$

where T_{ij} is the S-P time for the *i*th event at *j*th station. The S-P time was used to correct for geometrical spreading because some events located very close to some stations.

Receiver-function estimates for S waves

In frequency domain, the receiver-function corresponds to a simple division of the horizontal spectrum by the vertical one:

$$R(f) = H(f) / V(f) \quad (13)$$

Here, $H(f)$ is the spectrum of horizontal component as defined by (1), and $V(f)$ is the spectrum of vertical component. We calculated receiver-functions for S waves in frequency domain.

RESULTS AND DISCUSSION

Site effects

For site effects, we do not discuss the stations of FHS and CHE, because these two stations had only one record.

Site response from S-wave inversion method

Figure 2 shows the site amplification from the inversion of the S-wave spectra as a function of the frequency for each station. As shown in **Figure 2**, the stations at soil sites (LEI, MZZ, SMN, and DH0) have amplification effects at frequencies from 1 to 8 Hz, and the largest amplification value can be greater than 5. From the site responses for horizontal components, we can see that the frequency corresponding to the largest amplification values is about 2 Hz for LEI, MZZ and SMN. That is, it is 1.8 Hz for LEI, 1.8 Hz for MZZ and 2.2 Hz for SMN, respectively. For DH0, it is about 4 Hz. However, for the rock site station, XTS, the frequency characteristic of the site response is much more flat than that of those soil site stations. Its amplification values are close to one at low frequencies less than about 1 Hz, but they make small peaks and troughs at frequencies from 1 to 8 Hz.

We next make a comparison between the site responses from various techniques (direct spectral ratios of S and receiver-function of S waves) and those from the inversion of S-wave spectra.

Direct spectral ratios of S waves

Figure 3 shows the site amplification from direct spectral ratios of S waves as a function of the frequency for each station. For comparison, the result from the S-wave inversion is also shown. From this figure, we can see that there is a similarity in the shape of the site response curves from the two methods for each station, and the frequency of predominant peak of the site response from the direct spectral ratios agrees well with that from the inversion for each station. However, the amplification values from the spectral ratios are different from those from the inversion. For XTS, DH0 and LEI, the amplification values from the spectral ratios are larger than those from the inversion, but for MZZ and SMN, on the contrary, the amplification values from the spectral ratios are smaller than those from the inversion.

We compare the average amplifications at all stations from the spectral ratios and those at all stations from the inversion (**Fig. 4**). As shown in **Fig. 4**, in general, the average amplification values from the inversion method are larger than those from the spectral ratio method. But the two amplifications determined from both methods are well correlated within a factor of about 2. We did the same analysis as shown in **Fig. 4** for each site. The results are shown in **Fig. 5**. From this figure, we can see that the largest difference of amplification values between the two methods reaches up to about a factor of about 10 (for XTS and SMN). However, we can see also from the results around a predominant frequency of the site response for each site (similarly shown in **Fig. 4**) that the difference of amplification values between the two methods reduces within a factor of about 2 to 3 for

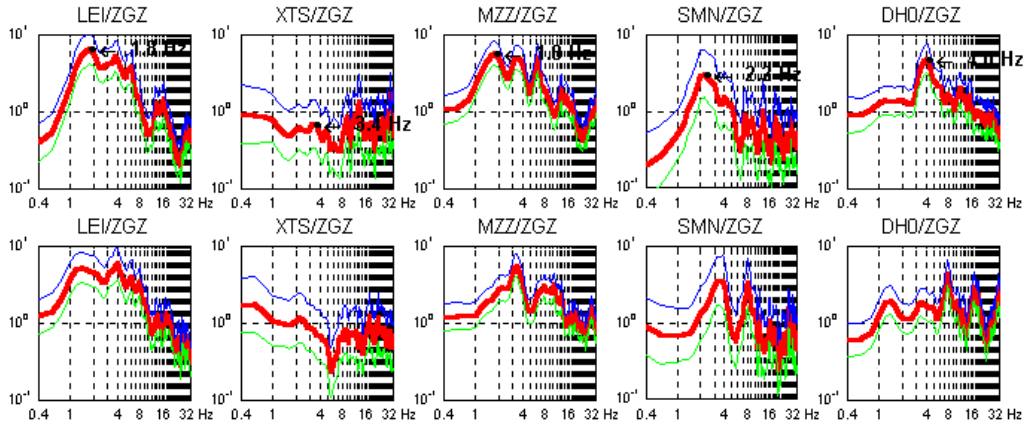

all stations (LEI: for 1.8 Hz, MZZ: for 1.8 Hz, SMN: for 2.2 Hz, XTS: for 3.4 Hz, and DH0: for 4.0 Hz). From the

Fig.2 Site response obtained from the inversion of the S-wave spectra using ZGZ rock station as a reference Site Upper is for the horizontal component and lower is for the vertical component. Thick lines represent the average, and thin lines represent ± one standard deviation of the site response.

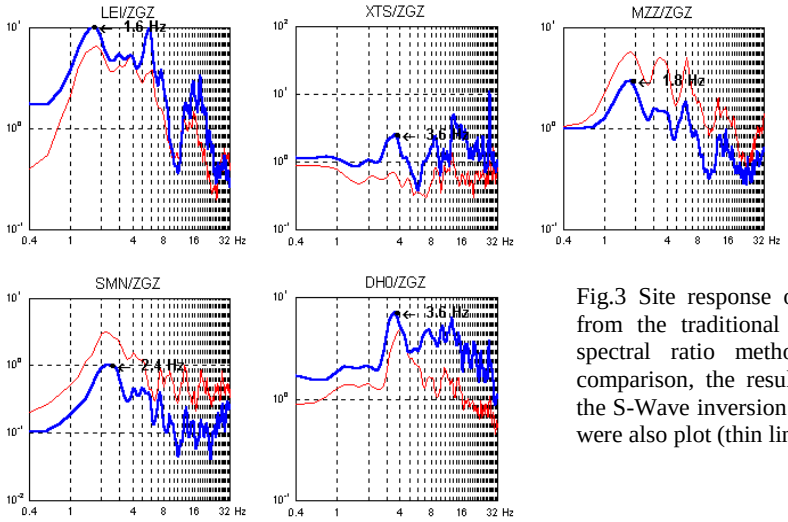

Fig.3 Site response obtained from the traditional S-wave spectral ratio method. For comparison, the results from the S-Wave inversion method were also plot (thin line)

Fig.4 Average amplification at all sites from traditional spectral ratios of S waves versus that

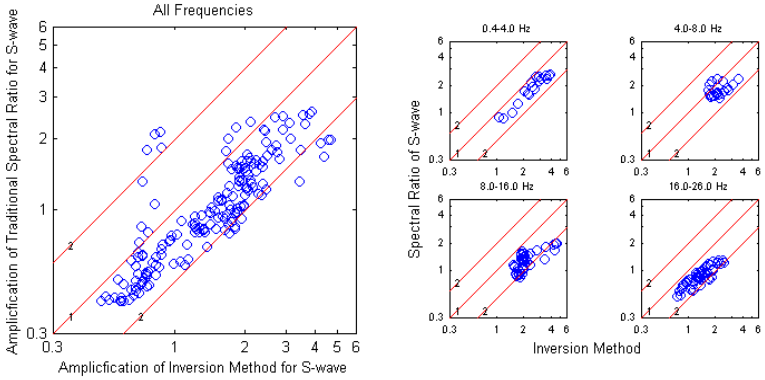

from the inversion method, lines represent a factor of difference between two methods.

above, we can say that the site amplifications obtained from the spectral ratio method are similar to those obtained from the inversion method within a factor of 2 to 3.

Here, it should be pointed out that the traditional spectral-ratio method for S waves has a weakness in our case, that is, many earthquakes occurred closely to the reference site, ZGZ. When we calculated the spectral ratios between a station and the reference station, we neglected the effect of wave attenuation due to absorption and scattering of seismic waves, that is Q_s^{-1}. The effect of attenuation, Q_s^{-1}, might play an important role in estimation of the site amplification for stations far from the earthquakes.

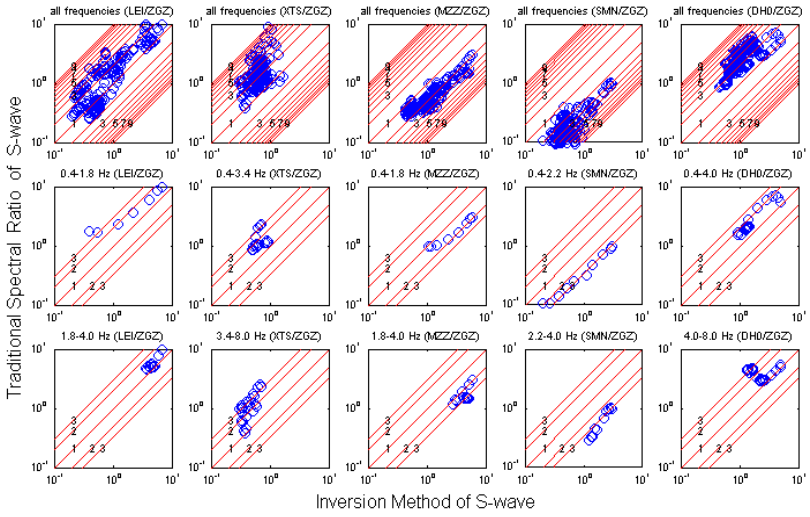

Fig. 5 Average amplification at each site from traditional spectral ratios of S waves versus that from the inversion method for all frequencies and around the predominate frequency

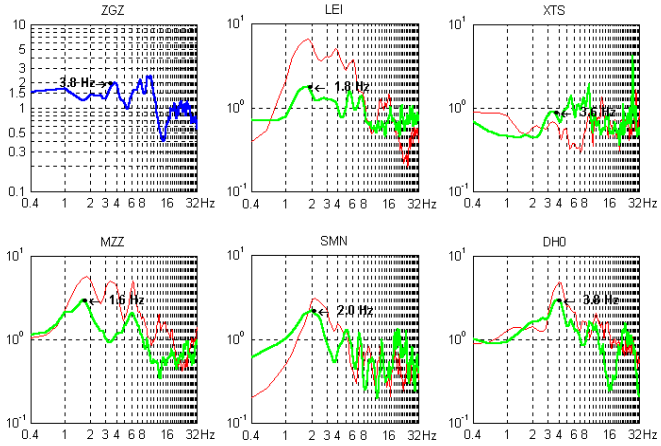

Fig. 6. Site response obtained from receiver-function (H/V ratio) for S waves. For comparison, the results from the inversion method were also plotted (thin line)

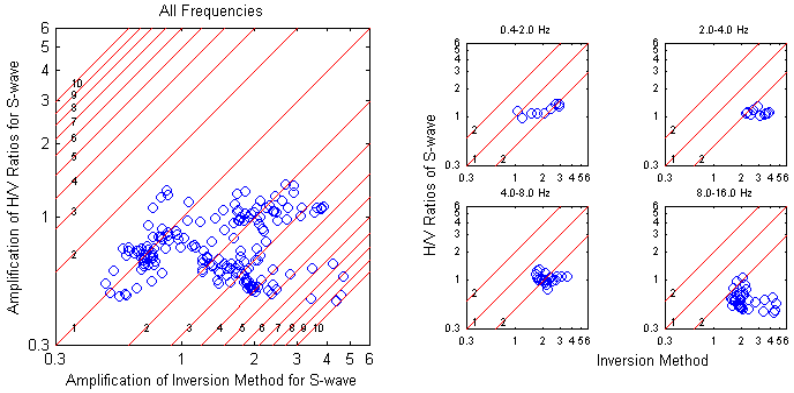

Fig. 7. Average amplification at all sites from receiver-function (H/V ratios) of S waves versus that from the inversion method.

Receiver-function for S waves

Figure 6 shows the site amplification from receiver-function for S waves as a function of the frequency for each station. For comparison, the result from the S-wave inversion is also shown. The frequency of predominant peak of the site response from the receiver-function is similar to that from the inversion for each station. However, the amplification values from the receiver-function are different from those from the inversion. We also calculated the average amplifications at all stations from the receiver-function method versus the average amplifications at all stations from the inversion method. The results are shown in **Figure 7.** From this figure, we can see that the amplification values obtained from the receiver-function method are smaller than those obtained from the inversion method and that the correlation between the amplifications from the receiver-function and those from the inversion is not good, especially at frequencies more than about 8 Hz. The difference between the amplifications from the receiver-function and those from the inversion becomes larger with the increase of frequency. Many researchers have also got the same result (Field and Jacob, 1995; Lachet et al., 1996; Bonilla et al, 1997). Their studies show that, in general, the resonance frequency obtained from the receiver-function method is statistically similar to that obtained from the inversion method; nevertheless, the amplification is very different from that of the inversion method.

In our case, the receiver-function of the reference site, ZGZ, is much more flat than that of the other sites, especially at low frequencies of 0.4 to 8 Hz, and the values of receiver-function are close to 1.5 at frequencies less than 3 Hz. This means that ZGZ is a good reference site among the stations used in the frequency range of 0.4 to 8 Hz. But the values of receiver-function for ZGZ are significantly unstable after 10 Hz. That implies, at these frequencies, the station maybe has its own site response.

Effect of propagation path

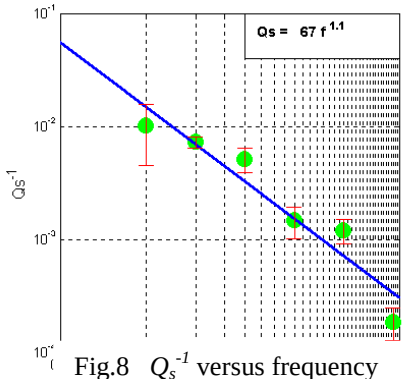

Fig.8 Q_s^{-1} versus frequency

Figure 8 shows the Q_s-values determined from the S-wave inversion method as a function of frequency. As shown in this figure, the Q_s-values are clearly in proportional to frequency. So, we here used a model $Q_s = \alpha f^{\beta}$ to fit the evaluated Q_s-values, and got the relation, $Q_s = 67\, f^{1.1}$, in the frequency range from 0.5 to 32 Hz. During the computation on Q_s-values, we tested the time-windows with several lengths to extract S waves in the lapse-time range from 2 to 10 seconds. From the tests, we found that the Q_s-values became unstable with the increase of length of time-window, especially at intermediate frequencies of 6 to 8 Hz. With the longer the signal segment involved, the more scattering and reflections are included in the signal. For moderate-sized or small-sized earthquakes, the main part of S waves is usually from 3 to 5 seconds. So, we used the time-windows with three lengths (3, 4 and 5 seconds) to calculate Q_s-values, and averaged the Q_s-values obtained from the three time-windows. However, the length of time-window has little effect on the calculations of the site amplification and source spectra. Thus, we used the 5-sec time-window to compute the site amplification and source spectra.

Source spectra

The inversion method solves for the source, Q_s and site term assuming that the response of the reference station is 1.0, independent of frequency. This assumption implies that the chosen station is a good site. However, the computed source spectra are implicitly convoluted with the site response of the reference station. Thus, if the reference site has its own frequency-dependent response, then this response is incorporated into the evaluated source spectrum when the response of the reference site is constrained to 1.0. We examine the source spectra evaluated from the inversion method from this point of view.

We preliminary examined the displacement source spectra by using the ω^{-2} model for seismic source. **Figure 9** shows the comparisons of the evaluated source spectra and the theoretical source models. From this figure, we found that the source spectra follow the ω^{-2} model for low frequencies less than about 12 Hz. For high frequencies more than about 12 Hz, however, the source spectra decrease rapidly compared with the theoretical

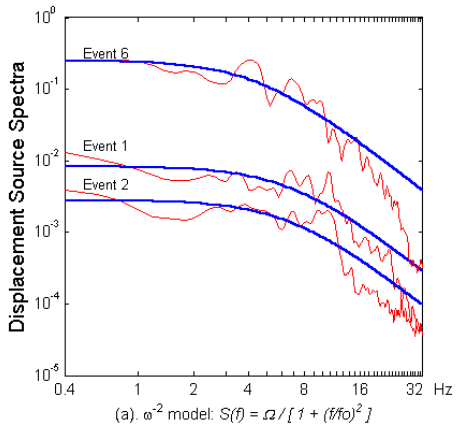

Fig.9 Some examples of preliminary results on displacement source spectra
Thick line is derived from theoretical spectra,
Thin line is obtained from the inversion method;
ω^{-2} model: $S(f) = \Omega/[1+(f/f_0)^2]$

source model. The decrease in high frequency of the source spectra is interpreted at least in part as amplification of the high frequencies at the reference site. After this, we need to examine its own response of the reference site using data observed at another rock site, XTS.

CONCLUSIONS

Seismic source, propagation path and site effects of Tangshan area, China, were evaluated by the S-wave inversion method using data from the strong-motion observation array. The site effects were also calculated by other techniques, such as direct spectral ratios of S waves and receiver-function of S waves. Then they were compared with the site response from the S-wave inversion. The main results are as follows.

(1). The S-wave quality factor, Q_s-value, is proportional to frequency in the range of 0.5 to 32 Hz, and it is approximately satisfied with the relation of $Q_s = 67\, f^{1.1}$ in Tangshan area, China.

(2). All the methods for site-effect estimation examined in this study can extract the same predominant peaks from the site responses for each soil site. The amplifications from direct S-wave spectral ratios are well correlated with those from the S-wave inversion within a factor of 2 to 3, while the correlation between the amplifications from S-wave receiver-function and those from the S-wave inversion is not good, especially for high frequencies more than 8 Hz.

(3). The source spectra of the ten events used in this study follow the ω^{-2} model of seismic source for low frequencies less than about 12 Hz.

ACKNOWLEDGMENTS

We would like to thank Professor Kojiro Irikura for his encouraging us in this study. In this study, RMIT Seismology Research Center, Australia supports two seismographs, Kelunji. This study was supported by Japan-China joint research on strong ground motion prediction and earthquake disaster mitigation.

REFERENCES

Andrews, D. J. (1982): Separation of source and propagation spectra of seven Mammoth Lakes aftershocks, *Proceedings of Workshop XVI, Dynamic characteristics of faulting, 1981, U.S. Geol. Sur. Open File Rep*..

Brune, J. N. (1970): Tectonic stress and the spectra of seismic waves from earthquakes, *J. Geophy. Res*., Vol. 75, pp. 4997-5009.

Field, E. H. and K. H. Jacob (1995): A comparison and test of various site response estimate techniques, including three are non reference-site dependent, *Bull. Seism. Soc. Am*., Vol. 85, pp. 1127-1143.

Iwata, T. and K. Irikura (1986): Separation of source, propagation and site effects from observed S-waves, *Zisin* II, Vol. 39, pp. 579-593 (in Japanese).

Kato. K., K. Aki, and M. Takemura (1995): Site amplification from coda waves: validation and application to S-wave site response, *Bull. Seism. Soc. Am*., Vol. 85, pp. 467-477.